Published in final edited form as:
Prog Biophys Mol Biol. 2008 ; 98(2-3): 161–170. doi:10.1016/j.pbiomolbio.2009.01.010.

Mathematical simulations of ligand-gated and cell-type specific effects on the action potential of human atrium

Mary M. Maleckar[a], **Joseph L. Greenstein**[a], **Natalia A. Trayanova**[a], and **Wayne R. Giles**[b,*]
[a]Department of Biomedical Engineering, Johns Hopkins University, Baltimore, MD 21218, USA
[b]Faculty of Kinesiology, University of Calgary, 2500 University Drive NW, Calgary, Alberta, Canada T2N 1N4

Abstract

In the mammalian heart, myocytes and fibroblasts can communicate via gap junction, or connexin-mediated current flow. Some of the effects of this electrotonic coupling on the action potential waveform of the human ventricular myocyte have been analyzed in detail. The present study employs a recently developed mathematical model of the human atrial myocyte to investigate the consequences of this heterogeneous cell–cell interaction on the action potential of the human atrium. Two independent physiological processes which alter the physiology of the human atrium have been studied. i) The effects of the autonomic transmitter acetylcholine on the atrial action potential have been investigated by inclusion of a time-independent, acetylcholine-activated K^+ current in this mathematical model of the atrial myocyte. ii) A non-selective cation current which is activated by natriuretic peptides has been incorporated into a previously published mathematical model of the cardiac fibroblast. These results identify subtle effects of acetylcholine, which arise from the nonlinear interactions between ionic currents in the human atrial myocyte. They also illustrate marked alterations in the action potential waveform arising from fibroblast–myocyte source–sink principles when the natriuretic peptide-mediated cation conductance is activated. Additional calculations also illustrate the effects of simultaneous activation of both of these cell-type specific conductances within the atrial myocardium. This study provides a basis for beginning to assess the utility of mathematical modeling in understanding detailed cell–cell interactions within the complex paracrine environment of the human atrial myocardium.

Keywords

Acetylcholine; Natriuretic peptides; Human atrium; Fibroblast; Mathematical model

1. Introduction

The mammalian myocardium is a functional syncytium: rapid and efficient cell–cell communication is essential for each heartbeat. This connexin-mediated electrotonic current flow between myocytes can modulate the excitability and the patterns of activation and subsequent contraction in both the atria and the ventricles. Often the complex and heterogeneous three-dimensional electrophysiological substrate in the mammalian heart is considered to be a homogeneous structure consisting mainly, or entirely, of cardiac myocytes. However, fibroblasts comprise 60–70% of the total cell number in the adult mammalian heart (Camelliti et al., 2005; Baudino et al., 2006). Recent immunohistochemical and

*Corresponding author. Tel.: +1 403 220 5607. wgiles@ucalgary.ca (W.R. Giles).

electrophysiological findings have demonstrated that fibroblast/myofibroblast cell populations within the mammalian heart can communicate electrotonically with myocytes, as well as with one another (Kamkin et al., 1999; Gaudesius et al., 2003; Kohl et al., 2005; Camelliti et al., 2005; Miragoli et al., 2006; Chilton et al., 2007; Cabo et al., 2008). This cell–cell interaction occurs via gap junction-mediated electrotonic coupling with the connexin family of integral membrane proteins playing a key role (Rook et al., 1992). Such functional communication appears to be dynamic and can change significantly in pathophysiological contexts (Brown et al., 2005), including both ischemic heart disease and metabolic syndromes. Recently, the functional consequences of electrotonic coupling between heterogeneous cell types on the electrophysiology of the myocyte have been investigated using mathematical models in which variable numbers of fibroblasts/myofibroblasts are coupled to selected numbers of myocytes (MacCannell et al., 2007; Sachse et al., 2008; Jacquemet and Henriquez, 2007, 2008). Collectively, these experimental and theoretical studies have drawn attention to the significant effects of this electrotonic coupling on myocyte excitability and action potential waveform in both the adult atrium and ventricle as well as in the neonatal myocardium (for review see Baudino et al., 2006; Cabo, 2008; Burstein and Nattel, 2008). Many of these effects arise from the source–sink relationships between the fibroblasts and myocytes. However, marked changes in intercellular resistance could also be a significant variable following both acute myocardial challenges (e.g., reperfusion following ischaemia) or longer-term events including gap junction remodeling and changes in intercellular Ca^{2+} or pH.

In the present study, a recently developed model of the human atrial action potential (Nygren et al., 1998; Maleckar et al., submitted for publication), and a mathematical formulation which can simulate atrial myocyte and fibroblast interactions (Maleckar et al., submitted for publication-b) has been utilized to further investigate fibroblast–atrial myocyte interactions during selected conditions known to be important for autonomic regulation and for paracrine modulation of atrial electrophysiology. These computations are based on recent experimental findings (Shibukawa et al., 2005; Chilton et al., 2007; Rose and Giles, 2008; Cabo, 2008) and were motivated in part by the classical work of Spach and his colleagues. These papers (Spach et al., 1981; Spach and Boineau, 1997) were among the first to draw attention to significant effects of fibroblasts and fibrosis on atrial electrophysiology. The present model extends previous work in two significant ways: i) the human atrial model includes the actions of the autonomic neurotransmitter acetylcholine (ACh) on the human atrium (cf. Demir et al., 1999; Kneller et al., 2002) and ii) a recently described, quasi-linear conductance which is activated by natriuretic peptides, and is localized to the fibroblast (Rose et al., 2007; Rose and Giles, 2008), has been included. Specifically, a mathematical model which can account for ACh-induced activation of a ligand-gated, inwardly rectifying, ACh-sensitive K^+ current, $I_{K(ACh)}$ has been incorporated (Kneller et al., 2002) into our model of the human atrial myocyte (Maleckar et al., submitted for publication-a). In addition, a nonselective cation conductance, activated by nanomolar concentrations of natriuretic peptide (Rose et al., 2007), has been included in the mathematical formulation for the fibroblast (Shibukawa et al., 2005; MacCannell et al., 2007). The resulting simulations illustrate the marked changes in resting potential, atrialmyocyte excitability, and action potential waveform which are caused by the direct actions of acetylcholine via $I_{K(ACh)}$. These computations also demonstrate the significant effects of natriuretic peptide-dependent activation of a ligand-gated conductance which is expressed only in the fibroblast.

Additional development of these types of integrative mathematical models will provide a useful complement to ongoing experimental work directed toward investigating the complex, but fundamental properties of the atrial syncytium, its autonomic innervation and its paracrine/autocrine environment. In this way mathematical modeling can, in principle, contribute to mechanistic investigations of atrial rhythm disturbances (Shiroshita-Takeshita et al., 2005; Van Wagoner and Nerbonne, 2000; Burstein and Nattel, 2008; Zlochiver et al., 2008).

2. Methods

Publications from our groups have included simulations based on reformulation and optimization of the K^+ currents which are responsible for action potential repolarization in the human ventricle (Fink et al., 2006, 2008), and the human atrium (Maleckar et al., submitted for publication-a). These models have been used as a basis for exploring the consequences of electrotonic coupling between a selected number of fibroblasts or myofibroblasts and a fixed number of human ventricular myocytes (MacCannell et al., 2007) or human atrial myocytes (Maleckar et al., submitted for publication-b).

The present study extends this theoretical analysis and model development while focusing on human atrial electrophysiology. Additional model development allows some of the direct effects of cholinergic autonomic innervation of the atrium (c.f. Pappano and Mubagwa, 1991; Imai et al., 2001; Shibata et al., 2006), and one aspect of the electrophysiological changes produced by the local paracrine and autocrine environments to be addressed (Oliver et al., 1997; Horio et al., 2003; D'Souza et al., 2004; Kuhn, 2004).

2.1. Mathematical model of the human atrial myocyte

The updated mathematical model of the human atrial myocyte action potential which is used in this study (Maleckar et al., submitted for publication-a) includes many of the fundamental aspects which were first developed within the adult human atrial myocyte model of Nygren et al. (1998, 2001). As was the case in the parent (1998) model, the biophysical descriptors of the electrophysiological properties of the atrial cell (electrical equivalent circuit for the sarcolemma) include ionic currents based on Hodgkin– Huxley formalisms, as well as a fluid compartment model to account for changes in ionic concentrations. The cylindrical dimensions and capacitance of the human atrialmyocyte are 11 μm (diameter) × 130 μm (length) and 50 pF, respectively.

Fig. 1A is a schematic of the human atrial myocyte model. It includes the main time- and voltage-dependent ion currents which contribute to the generation of the human atrial action potential: I_{Na}, $I_{Ca,L}$, I_t, I_{kur}, I_{K1}, I_{Kr}, and I_{Ks}. This model also includes electrogenic pump and exchanger currents: the sarcolemmal Ca^{2+} pump current ($I_{Ca,P}$), the Na^+–Ca^{2+} exchanger current (I_{NaCa}), and the Na^+–K^+ pump current (I_{NaK}). These transporters are responsible for the maintenance of intracellular ion concentrations, and are balanced by Na^+ and Ca^{2+} time-independent or background currents, I_{BNa} and I_{BCa}.

The computations in the present paper utilize our recently developed model of the human atrial action potential (Maleckar et al., submitted for publication-a). A significant motivation for developing this model was to provide a more accurate reconstruction of the repolarization of the atrial action potential at a number of different steady-state frequencies of stimulation. Previous models had only limited success in this important application (Nygren et al., 1998; Courtemanche et al., 1998; Ramirez et al., 2000). Significant improvements in mathematical reconstruction of atrial action potential repolarization are now possible as a result of quite comprehensive experimental studies done on human atrial tissue and isolated myocytes from human atrium (c.f. Nattel and Opie, 2006). For example, in our recent model (Maleckar et al., submitted for publication-a) both the transient outward K^+ current, I_t, and the ultra rapid delayed rectifier (sustained outward) K^+ current, I_{kur}, were significantly reformulated based on additional experimental findings (Fedida et al., 1993, Amos et al., 1996; Dawodu et al., 1996; Feng et al., 1998; Dobrev et al., 2001; Wang et al., 2003; Gaborit et al., 2007).

In fact the original formulation of I_t (Shibata et al., 1989; Nygren et al., 1998) was based on rabbit atrial myocyte experimental data. It is now known that the voltage-gated K^+ channel underlying I_t in the rabbit atrium is the Kv1.4 gene product. In contrast, in human atrium the

α-subunit of this channel is encoded by Kv4.3 (Fermini et al., 1992; Wang et al., 2003, 2005). This change is very important since both the inactivation and the reactivation properties of Kv1.4 differ dramatically from those of Kv4.3 (for details see Maleckar et al., submitted for publication-a).

The equations describing another important repolarizing K^+ current were also changed significantly. This so-called rapidly delayed rectifier, I_{kur}, is encoded by the voltage-gated K^+ channel α-subunit Kv1.5 (Fedida et al.,1993). It activates very rapidly (<10 ms) (Amos et al., 1996) but inactivates very slowly (~3 s). In (Nygren et al., 1998) both the inactivation and recovery of this current had kinetics which were an order of magnitude more rapid than were observed in subsequent experiments. Accordingly, I_{Kur} was completely reformulated in our present model (Maleckar et al., submitted for publication-a).

The formulations of all remaining currents, ion fluxes, and Ca^{2+} homeostasis mechanisms were identical to those described previously (Nygren et al., 1998). In addition, the model of the human atrial myocyte employed in this study has eliminated the electro-neutral Na^+ influx, Φ_{en}, of the model of Nygren et al. (Nygren et al., 1998) in order to achieve long-term stability in ionic concentrations over long periods of stimulation. A consequence of the incorporation of $\Phi_{en}$was a lack of charge conservation, as well as the absence of any true mathematical steady states (Jacquemet, 2007). The stimulus current delivered to the intracellular space is now attributed to the movement of K^+ ions, as suggested by Hund et al. (2001) rather than balanced by the inclusion of Φ_{en}. As a result, charge is conserved within the system for any stimulation protocol.

2.2. Acetylcholine-activated K^+ current $I_{K(ACh)}$

An acetylcholine-activated K^+ current ($I_{K(ACh)}$) was incorporated into the present model of the human atrial myocyte, as has been done previously in a number of different mathematical models of the mammalian myocardium (cf. Demir et al., 1999) this addition is shown in bold and indicated by the ellipse in Fig. 1A. The mathematical formulation which we have utilized was the one in Kneller et al. (2002). Fig.1B consists of two steady-state current–voltage (*I–V*) relationships for $I_{K(ACh)}$. These *I–V* curves illustrate the current density of $I_{K(ACh)}$ within physiological voltage ranges for two representative concentrations of acetylcholine [ACh]. In the present study, [ACh] was varied systematically over two orders of magnitude in an attempt to simulate dose–response effects on the atrial myocyte action potential and resting potential. In any given simulation [ACh] was assumed to be at a fixed level of 0.03, 0.15, 0.3, 0.6, 1.5, or 3 μM. This range corresponds approximately to the experimental conditions in which carbamylcholine (CBC), a stable analogue of acetylcholine was applied at concentrations of 1, 5, 10, 20, 50, and 100 nM (Kneller et al., 2002).

2.3. Na^+ current, I_{Na}

The peak magnitude of I_{Na} was increased in Maleckar et al. (submitted for publication-a) human atrial myocyte model by 12.5% to be consistent with experimental measurements of the maximum upstroke velocity of the human atrial action potential (Dawodu et al., 1996). The voltage dependence of the steady-state activation and inactivation of I_{Na} is presented in Fig. 1C. These biophysical descriptors are important for this paper because modulation of the myocyte resting membrane potential, following [ACh] treatment and/or coupling to fibroblasts, significantly alter myocyte excitability (see Fig. 3). In the human atrium, the resting potential, approximately −70 mV. As a result a significant fraction of the Na^+ current is inactivated at this physiological membrane potential.

2.4. Fibroblast–myocyte coupling

A schematic of fibroblast–myocyte electrotonic coupling is shown in Fig. 2A. All simulations which investigated the effects of electronic coupling were done assuming that a single fibroblast with a capacitance of 6.3 pF (Shibukawa et al., 2005)was coupled to one myocyte. A fixed gap junctional coupling conductance (G_{gap}) of 0.5 nS was assumed (Rook et al., 1992; c.f. Baudino et al., 2006;MacCannell et al., 2007). More details of the way in which we have formulated this cell–cell interaction model are presented in Maleckar et al. (submitted for publication-b).

In brief, the electrophysiological properties of the fibroblast membrane are represented by a model adapted very similarly to that developed by MacCannell et al. (2007). This model employs five time- and voltage-dependent active membrane conductances, as shown in Fig. 2B. For the purposes of this study, a ligand-gated non-selective cation current which is activated by natriuretic peptides (NP) in cardiac fibroblasts was simulated (see Rose et al., 2007). To explore the effects of this quasi-linear conductance the NP activated current (I_{NP}) was incorporated into the ionic model of the fibroblast, as indicated by the dashed ellipse in Fig. 2B. The *I–V* relationship of this time-independent current is essentially linear in the range of physiological potentials (Rose et al., 2007). I_{NP} was therefore modeled as:

$$I_{NP}=g_{NP}(V_{Fb}-E_{NP})$$

where g_{NP} is a constant conductance equal to 1.25 nS, V_{Fb} is the transmembrane potential of the fibroblast, and E_{NP} is the reversal potential of the channel, experimentally found to be approximately 0 mV. The *I–V* relationship of this time-independent, linear fibroblast conductance is shown in Fig. 2C.

2.5. Simulation protocol and data analysis

In a typical simulation one atrial myocyte was subjected to a selected [ACh] corresponding to 0 (control), 1, 5, 10, 20, 50, or 100 nM. Ten stimuli were applied at 1 Hz using a stimulus current of −6.2 pA/pF for 5 ms. Measurements of resting membrane potential (RMP), dV/dt_{max}, action potential amplitude (APA), and action potential duration at 90% repolarization (APD_{90}) were then performed. These parameters were used to construct the dose– response curves as shown in Results.

All simulations of electrotonic coupling assumed a one-to-one myocyte-to-fibroblast coupling ratio and a fixed intercellular conductance of 0.5 nS. Control conditions were defined and are illustrated based on coupling between a myocyte and a fibroblast in the absence of both ACh and NP. Simulations also investigated the effects of coupling between a single atrialmyocyte and fibroblast in the presence of natriuretic peptides (NP), or in the presence of both ACh and NP. The myocyte was again subjected to a selected concentrations of [ACh] and an identical train of 10 stimuli was applied. In these simulations a 1.5× threshold stimulus current (−5.6 pA/pF for 5 ms) was utilized. Measurements of resting membrane potential (RMP) were then performed and used to construct dose–response curves for [ACh].

3. Results

3.1. Effects of acetylcholine on human atrial action potential waveform

The six panels in Fig. 3 show output from action potential simulation (1.2 × threshold, at 1 Hz steady state) in which the effects of acetylcholine, (ACh) is applied. This autonomic transmitter results in instantaneous activation of a weakly inwardly rectifying K^+ current, $I_{K(ACh)}$, as shown in Fig. 1B. The main electrophysiological effect of ACh is the presence of an additional

outward current at all membrane potentials positive to approximately −70 mV. This outward current would be expected to: i) hyperpolarize the resting potential, RMP, and ii) shorten the action potential duration, APD. Fig. 3 demonstrates that both of these effects are observed, and within limits, both of these effects scale progressively with increasing ACh concentrations. Concentration-dependent ACh-induced effects on the RMP, action potential duration at the point of 90% repolarization (APD_{90}), and action potential amplitude (APA) are shown/summarized in Fig. 3, Panels C, E and F, respectively.

Note that the ACh-induced effects on myocyte excitability (shown in Panels B and D) are somewhat unexpected. The two superimposed traces in Panel B demonstrate that ACh (10 nM) causes a delay in the initiation of the action potential in this isolated '*in silico*' human atrial myocyte. This delay arises largely from the instantaneously activated outward current due to $I_{K(ACh)}$. This effectively reduces the ability of the stimulus current to charge the myocyte to the threshold membrane potential. The ACh-induced small hyperpolarization of the RMP is also a contributing factor for the increased latency to action potential initiation.

Careful inspection reveals that the ACh-induced effects on atrial myocyte excitability and action potential waveform are complex. In part, this complexity arises from concentration dependent but diverse effects on key electrophysiological parameters. As illustrated in Fig. 3D the maximum rate of rise of the action potential increases as ACh concentration is raised in the range approximately 1–50 nM. This is because the ACh-induced hyperpolarization of the RMP removes steady-state inactivation of I_{Na} (see Fig. 1, Panel C). This 'hyperexcitability', however, is strongly concentration dependent. At ACh concentrations larger than approximately 50 nM, the outward current ($I_{K(ACh)}$) which is present in the range of membrane potentials close to the excitability threshold has a very strong influence. The net effect is an increased latency to firing and reduced excitability, sometimes including failure of this stimulus paradigm to produce an action potential, in spite of the hyperpolarization of the RMP.

3.2. Effects of acetylcholine on a minimal atrial functional syncytium: one myocyte coupled to one fibroblast

The next set of simulations was done to explore the changes in thehumanatrial action potential waveform in the presence of 10 nM ACh when one myocyte was coupled to one fibroblast through a coupling conductance at 0.5 nS. The 3 superimposed traces in Panel A of Fig. 4 illustrate these changes in action potential waveform. The solid black trace repeats data shown in Fig. 3, for reference. The dashed lines show the change in resting potential and action potential waveform when the fibroblast is coupled through a gap conductance of 0.5 nS. Note that there are 3 significant changes: (i) a depolarization of the myocyte resting potential, (ii) a decrease in the action potential duration (APD) during early repolarization and (iii) a lengthening of APD during late repolarization.

The addition of ACh (10 nM), generates an outward current at all physiological membrane potentials. This has the expected effects: the resting membrane potential hyperpolarizes and the action potential in the coupled atrial myocyte shortens substantially. It is of interest to understand the changes in the electrophysiological status of the passive cell, the fibroblast in this syncytium. As shown in Fig. 4B the control resting potential in the uncoupled fibroblast is (approximately) −40 mV. This Figure also shows the substantial electrotonic depolarization of the membrane potential in the coupled fibroblast in response to each action potential in the myocyte. In this panel the dashed line depicts the electrotonic changes in membrane potential in the fibroblast under control conditions (no ACh), while the data depicted by the red line illustrates these changes in the presence of 10 nM ACh.

Fig. 4C shows the trans-gap current flow corresponding to the 3 sets of conditions in Panel 4A. The plot in Panel 4D focuses on the change in resting potential of the myocyte in the two

conditions of interest. Note that under these conditions, the inward current generated by the relatively depolarized fibroblast tends to depolarize the restingmembrane potential of themyocyte. In summary the main effect of the coupled fibroblast is to reduce or remove the hyperpolarization in the myocyte which is caused by the activation of $I_{K(ACh)}$ (c.f. Boyett et al., 1995;Christ et al., 2008).

3.3. Natriuretic peptide effects on the atrial fibroblast

The final set of simulations was done to begin to explore the interactions between autonomic tone (an effect of ACh) on the myocyte, and one aspect of the paracrine environment in the atrium – an electrophysiological effect of atrial natriuretic peptides. This effect is localized to the atrial fibroblast but, in principle, would be expected to alter myocyte electrophysiological properties as a result of connexin-mediated electrotonic current flow. In Fig. 5A, 2 of the 3 traces are analogous to those in Fig. 4A. Note, however, that the effect of the ligand-gated current, I_{NP}, which is activated only in the fibroblast tends to counteract the direct action of ACh in the myocyte. Under these conditions the net result is a marked depolarization of the myocyte resting membrane potential, and a pronounced action potential lengthening during the final repolarization phase. This is because the natriuretic peptide-induced current in the fibroblast is relatively large and net inward in the range of membrane potentials negative to its reversal potential which lies between −20 and 0 mV.

Panel B of Fig. 5 shows the effect on the fibroblast of the ligand-gated current due to the natriuretic peptide. This is a marked depolarization of the fibroblast. The corresponding changes in gap junction currents are shown in Fig. 5C. The plot in Fig. 5D shows that under the conditions of these computations, the ligand-gated natriuretic peptide-induced current in the fibroblast, I_{NP} strongly reduces and then overcomes the hyperpolarizing effect of ACh at all ACh concentrations (1–100 nM) that were ‘tested’.

4. Discussion

This study has utilized our recently developed mathematical models of the human atrial myocyte and fibroblast (Maleckar et al., submitted for publication-a–b). In the present study cell–cell electrotonic interactions, as well as cell-specific effects of ligand-gated ion channels, are explored. As shown in Fig. 3– Fig. 5 concentration-dependent effects of the autonomic transmitter, acetylcholine, (ACh), on the human atrial action potential can be reproduced by our mathematical formulation. In this study and in previous work ACh activates an inwardly rectifying, time-independent K^+ current, $I_{K(ACh)}$ (cf. Demir et al.,1999; Boyett et al.,1995; Kneller et al., 2002). This outward current hyperpolarizes the resting membrane potential (RMP) and markedly shortens the action potential duration (APD) in the human atrium. In addition to this validation, our computations also replicate less well-known ACh effects. For example a delay in the initiation of the action potential upstroke is revealed and this is consistent with acetylcholine causing ‘hyper-excitability’ in selected tissues within the healthy mammalian myocardium (Kawara et al., 2001). This effect is mainly due to the reduction in the *net* inward stimulus current as a consequence of activation of the outward current, $I_{K(ACh)}$. However, the hyperpolarization of the atrial RMP also contributes. Although this moves the resting membrane potential away from the action potential threshold; this hyperpolarization can cause a significant increase in excitability as a result of removal of inactivation of the Na^+ current, INa in the human atrium.

A main goal of our study was to further investigate the electrotonic interactions between myocytes and fibroblasts within the normal or healthy adult human atrium (Maleckar et al., submitted for publication-b; Camelliti et al., 2005; Kamkin et al., 1999; Jacquemet and Henriquez, 2007). Our initial work has assumed a fixed 1:1 coupling ratio (myocyte/fibroblast) as well as a fixed intercellular conductance of 0.5 nS. These conditions were chosen in part,

as a consequence of our experience with applying similar mathematical models of the human ventricular or atrial myocytes (c.f Nygren et al., 2001) coupled to selected numbers of fibroblasts (MacCannell et al., 2007; Maleckar et al., submitted for publication-b). As shown in Fig. 3 and Fig. 4 in the human atrium (as opposed to ventricle), electrotonic coupling to *even* one fibroblast was that the atrial myocyte resting potential depolarized significantly. In addition, the atrial myocyte action potential duration showed a marked shortening. The depolarization of the myocyte resting potential is driven by: i) the depolarized resting potential of the fibroblast (approximately −40mV), so that the myocyte–fibroblast difference in membrane potential acts as a current source. ii) The relatively high input resistance of the atrial myocyte, which results in even small currents causing substantial changes in resting membrane potential and action potential waveform (Joyner, 1982; Joyner and van Capelle, 1986; Joyner et al., 2000, 2007). The observed action potential shortening in themyocyte can be attributed in part to the current sink effect of the coupled fibroblast. Thus, during the action potential plateau in the myocyte, the fibroblast functions as a powerful current sink due to its time and voltage-dependent outward K^+ conductances.

The inclusion of a natriuretic peptide-activated non-specific cation conductance, I_{NP}, in the fibroblast results in an enhanced capability of the coupled fibroblast to serve as a current source within the physiological range of membrane potentials. This conductance, which was modeled based on recent experimental data from our laboratory (Rose et al., 2007; Rose and Giles, 2008), is an essentially linear, non-selective cation current with a reversal potential near 0 mV. As a result, at membrane potentials negative to 0 mV, I_{NP} generates an inward current that can significantly depolarizes the resting membrane potential of the fibroblast and thence the myocyte. At strongly depolarized membrane potentials (>0 mV), however, I_{NP} is an outward current, and this promotes repolarization of the fibroblast, and enhances the ability of the fibroblast to serve as a current sink.

Our computations, although still very preliminary, serve as a basis for beginning to investigate, using mathematical modeling, the complex chemical (neurotransmitter, endogenous peptide) and electrophysiological interactions that take place in the heterogeneous atrial myocardium. Despite the fact that only the *direct* electrophysiological effects of ACh (activation of $I_{K(ACh)}$) in the myocyte and the fibroblast-specific effects of natriuretic peptides were considered, the effects on action potential waveform are complex, in part due to nonlinear interactions between $I_{K(ACh)}$ and I_{NP}. These relationships can be explored further by more complete characterization of the concentration-dependent effects of $I_{K(ACh)}$ and I_{NP} in the context of fibroblast–myocyte coupling.

4.1. Limitations of this model

We recognize that the present model has limitations which must be considered when using it even for integrative purposes. These arise from (i) initial assumptions used in model development, (ii) incomplete experimental data in some important areas, and (iii) the intrinsic (but incompletely characterized) heterogeneity of the adult mammalian atrium. We note that:

1. All of our simulations have been done assuming a 1:1 fibroblast to myocyte coupling ratio. There is no experimental data which can be used to justify this assumption. However, the relatively strong electrotonic effects of a single fibroblast seen in the results indicate that this ratio to be appropriate for use in this study. The classical experimental work of Spach et al. (1997) did draw attention to effects of ‘microfibrosis’ on atrial electrophysiology.
2. The choice of the one myocyte/one fibroblast coupling paradigm employed in this study, has the consequence that the known heterogeneities in the atrial action potential and cholinergic innervation of the atria have not been accounted for (Allessi et al.,

1958; Ninomiya,1966; Li et al., 2001; Lomax et al., 2003; Gaborit et al., 2007). These differences are known to be mainly due to heterogeneous expression of K^+ currents, including $I_{K(ACh)}$, in the myocyte in different regions of the mammalian atria. These could be simulated by appropriate scaling of these currents in an additional study focusing on this atrial heterogeneity.

3. The cell-coupling paradigm of the present model is also limited by its failure to account for the electrophysiological effects of the extracellular matrix *per se*in the human atrium as well as the lack of inclusion of stretch-induced effects on either the fibroblast or the myocyte.

4. The present model does not incorporate any sophisticated formalisms for Ca^{2+} homeostasis in either the myocyte or the fibroblast. As a result changes in intracellular Ca^{2+} are not simulated accurately. Future studies of constitutive excitation–secretion coupling in the myocyte and coupled fibroblast will require further development of equations for Ca^{2+} transport, intracellular buffering and Ca^{2+}-induced Ca^{2+} release. The electrogenic current due to Na+/Ca^{2+} exchange is known to modulate the contour of final repolarization in the mammalian atrial action potential.

These and other considerations will need to be taken into account before this model or others similar to it can be used for perhaps two of their most important applications: analysis of mechanisms of antiarrhythmic drugs which act selectively on the atrium (Rampe et al., 1993; Feng et al., 1997; Seti et al., 1999; Blaaw et al., 2007; Christ et al., 2008); or detailed analysis of the ways in which changes in or remodeling of expression levels of K^+ currents can contribute to or account for atrial flutter or fibrillation (Schuessler et al., 1992; Brandt et al., 2000; Van Wagoner and Nerbonne, 2000; Burashnikov and Antzelevitch, 2006; Blaauw et al., 2007; Pijnappels et al., 2007; Burstein and Nattel, 2008).

Acknowledgments

The authors gratefully acknowledge support of this work by NIH grants R01-HL063195, R01-HL082729 and R01-HL067322, and NSF grant CBET-0601935 (Dr. N.A. Trayanova). The Giles laboratory is funded by the Canadian Institutes of Health Research and the Heart and Stroke Foundation of Canada. In addition, W. Giles holds a Medical Scientist Award from the Alberta Heritage Foundation for Medical Research.

References

Amos GJ, Wettwer E, Metzger F, Li Q, Himmel HM, Ravens U. Differences between outward currents of human atrial and subepicardial ventricular myocytes. J. Physiol 1996;491(Pt 1):31–50. [PubMed: 9011620]

Allessi R, Nusynowitz M, Abildskov JA, Moe GK. Nonuniform distribution of vagal effects on dog atria. Circ. Res 1958;194:406–410.

Blaauw Y, Schotten U, van Hunnik A, Neuberger HR, Allessie MA. Cardioversion of persistent atrial fibrillation by a combination of atrial-specific and non-specific class III drugs in the goat. Cardiovasc. Res 2007;75:89–98. [PubMed: 17466958]

Baudino TA, Carver W, Giles W, Borg TK. Cardiac fibroblasts: friend or foe? Am. J. Physiol. Heart Circ. Physiol 2006;291:H1015–H1026. [PubMed: 16617141]

Brandt MC, Priebe L, Bohle T, Sudkamp M, Beuckelmann DJ. The ultra rapid and transient outward K $^+$ current in human atrial fibrillation. Their possible role in post operative atrial fibrillation. J. Mol. Cell Cardiol 2000;32:1885–1896. [PubMed: 11013132]

Brown RD, Ambler SK, Mitchell MD, Long CS. The cardiac fibroblast: therapeutic target in myocardial remodeling and failure. Annu. Rev. Pharmacol. Toxicol 2005;45:657–687. [PubMed: 15822192]

Boyett MR, Kodama I, Honjo H, Arai A, Suzuki R, Toyama J. Ionic basis of the chronotropic effect of acetylcholine on the rabbit sinoatrial node. Cardiovasc. Res 1995;29:867–878. [PubMed: 7656291]

Burashnikov A, Antzelevitch C. Late-phase 3 EAD. A unique mechanism contributing to initiation of atrial fibrillation. PACE 2006;29:290–295. [PubMed: 16606397]

Burstein B, Nattel S. Atrial fibrosis: mechanisms and clinical relevance in atrial fibrillation. J. Am. Coll. Cardiol 2008;51:802–809. [PubMed: 18294563]

Cabo C. Modulation of impulse propagation by fibroblasts. Am. J. Physiol. Heart Circ. Physiol 2008;294:H1992–H1993. [PubMed: 18359897]

Camelliti P, Borg TK, Kohl P. Structural and functional characterization of cardiac fibroblasts. Cardiovasc. Res 2005;65:40–51. [PubMed: 15621032]

Chilton L, Giles WR, Smith GL. Evidence of intercellular coupling between co-cultured adult rabbit ventricular myocytes and myofibroblasts. J. Physiol 2007;583:225–236. [PubMed: 17569734]

Christ T, Wettwer E, Voigt N, Hala O, Radicke S, Matschke K, Varro A, Dobrev D, Ravens U. Pathology-specific effects of the $I_{Kur}/I_{to}/I_{K,ACh}$ blocker AVE0118 on ion channels in human chronic atrial fibrillation. Br. J. Pharmacol 2008;154:1619–1630. [PubMed: 18536759]

Courtemanche M, Ramirez RJ, Nattel S. Ionic mechanisms underlying human atrial action potential properties: insights from a mathematical model. Am. J. Physiol 1998;275:H301–H321. [PubMed: 9688927]

Dawodu AA, Monti F, Iwashiro K, Schiariti M, Chiavarelli R, Puddu PE. The shape of human atrial action potential accounts for different frequency-related changes in vitro. Int. J. Cardiol 1996;54:237–249. [PubMed: 8818747]

Demir SS, Clark JW, Giles WR. Parasympathetic modulation of sinoatrial node pacemaker activity in rabbit heart: a unifying model. Am. J. Physiol 1999;276:H2221–H2244. [PubMed: 10362707]

D'Souza SP, Davis M, Baxter GF. Autocrine and paracrine actions of natriuretic peptides in the heart. Pharmacol. Ther 2004;101:113–129. [PubMed: 14761702]

Dobrev D, Graf E, Wettwer E, Himmel HM, Hala O, Doerfel C, Christ T, Schuler S, Ravens U. Molecular basis for downregulation of G-protein-coupled inward rectifying K^+ current (IK,ACh) in chronic human atrial fibrillation: decrease in GIRK4 mRNA correlates with reduced IK,ACh and muscarinic receptor-mediated shortening of action potentials. Circulation 2001;104:2551–2557. [PubMed: 11714649]

Fedida D, Wible B, Wang Z, Fermini B, Faust F, Nattel S, Brown AM. Identity of a novel delayed rectifier current from human heart with a cloned K^+ channel current. Circ. Res 1993;73:210–216. [PubMed: 8508531]

Feng J, Xu D, Wang Z, Nattel S. Ultrarapid delayed rectifier current inactivation in human atrial myocytes: properties and consequences. Am. J. Physiol 1998;275:H1717–H1725. [PubMed: 9815079]

Feng J, Wang Z, Li GR, Nattel S. Effects of class III antiarrhythmic drugs on transient outward and ultra-rapid delayed rectifier currents in human atrial myocytes. J. Pharmacol. Exp. Ther 1997;281:384–392. [PubMed: 9103521]

Fermini B, Wang Z, Duan D, Nattel S. Differences in rate dependence of transient outward current in rabbit and human atrium. Am. J. Physiol 1992;263:H1747–H1754. [PubMed: 1481900]

Fink M, Giles WR, Noble D. Contributions of inwardly-rectifying K^+ currents to repolarization assessed using mathematical models of human ventricular myocytes. Philos. Trans. A: Math. Phys. Eng. Sci 2006;364:1207–1222.

Fink M, Noble D, Virag L, Varro A, Giles WR. Contributions of HERG K+ current to repolarization of the human ventricular action potential. Prog. Biophys 2008;96:357–376.

Gaborit N, Le Bouter S, Szuts V, Varro A, Escande D, Nattel S, Demolombe S. Regional and tissue specific transcript signatures of ion channel genes in the non-diseased human heart. J. Physiol 2007;582:675–693. [PubMed: 17478540]

Gaudesius G, Miragoli M, Thomas SP, Rohr S. Coupling of cardiac electrical activity over extended distances by fibroblasts of cardiac origin. Circ. Res 2003;93:421–428. [PubMed: 12893743]

Horio T, Tokudome T, Maki T, Yoshihara F, Suga S, Nishikimi T, Kojima M, Kawano Y, Kangawa K. Gene expression, secretion, and autocrine action of C-type natriuretic peptide in cultured adult rat cardiac fibroblasts. Endocrinology 2003;144:2279–2284. [PubMed: 12746286]

Hund TJ, Kucera JP, Otani NF, Rudy Y. Ionic charge conservation and long-term steady state in the Luo-Rudy dynamic cell model. Biophys. J 2001;81:3324–3331. [PubMed: 11720995]

Imai Y, Jiang B, Pappano AJ. Mechanism for muscarinic inhibition of I(Ca(L)) is determined by the path for elevating cyclic AMP in cardiac myocytes. Cardiovasc. Res 2001;51:331–343. [PubMed: 11470473]

Jacquemet V. Steady-state solutions in mathematical models of atrial cell electrophysiology and their stability. Math. Biosci 2007;208:241–269. [PubMed: 17174351]

Jacquemet V, Henriquez CS. Modelling cardiac fibroblasts: interactions with myocytes and their impact on impulse propagation. Europace 2007;9:v129–v137.

Jacquemet V, Henriquez CS. Loading effect of fibroblast-myocyte coupling on resting potential, impulse propagation and repolarization: insights from a microstructure model. Am. J. Physiol. Heart Circ. Physiol 2008;294:H2040–H2052. [PubMed: 18310514]

Joyner RW. Effects of the discrete pattern of electrical coupling on propagation through an electrical syncytium. Circ. Res 1982;50:192–200. [PubMed: 7055854]

Joyner RW, van Capelle FJ. Propagation through electrically coupled cells. How a small SA node drives a large atrium. Biophys. J 1986;50:1157–1164. [PubMed: 3801575]

Joyner RW, Wang YG, Wilders R, Golod DA, Wagner MB, Kumar R, Goolsby WN. A spontaneously active focus drives a model atrial sheet more easily than a model ventricular sheet. Am. J. Physiol. Heart Circ. Physiol 2000;279:H752–H763. [PubMed: 10924075]

Joyner RW, Wilders R, Wagner MB. Propagation of pacemaker activity. Med. Biol. Eng. Comput 2007;45:177–187. [PubMed: 16951930]

Kamkin A, Kiseleva I, Wagner KD, Lammerich A, Bohm J, Persson PB, Gunther J. Mechanically induced potentials in fibroblasts from human right atrium. Exp. Physiol 1999;84:347–356. [PubMed: 10226175]

Kawara T, Derksen R, de Groot JR, Coronel R, Tasseron S, Linnenbank AC, Hauer RN, Kirkels H, Janse MJ, Bakker JM. Activation delay after premature stimulation in chronically diseased human myocardium relates to the architecture of interstitial fibrosis. Circulation 2001;104:3069–3075. [PubMed: 11748102]

Kneller J, Zou R, Vigmond E, Wang Z, Leon LJ, Nattel S. Cholinergic atrial fibrillation in a computer model of a two-dimensional sheet of canine atrial cells with realistic ionic properties. Circ. Res 2002;17:E73–E87. [PubMed: 12016272]

Kohl P, Camelliti P, Burton FL, Smith GL. Electrical coupling of fibroblasts and myocytes: relevance for cardiac propagation. J. Electrocardiol 2005;38:45–50. [PubMed: 16226073]

Kuhn M. Molecular physiology of natriuretic peptide signalling. Basic Res. Cardiol 2004;99:76–82. [PubMed: 14963665]

Li D, Zhang L, Kneller J, Nattel S. Potential ionic mechanism for repolarization differences between canine right and left atrium. Circ. Res 2001;88:1168–1175. [PubMed: 11397783]

Lomax AE, Rose RA, Giles WR. Electrophysiological evidence for a gradient of G protein-gated K+ current in adult mouse atria. Br. J. Pharmacol 2003;140:576–584. [PubMed: 14522844]

MacCannell KA, Bazzazi H, Chilton L, Shibukawa Y, Clark RB, Giles WR. A mathematical model of electrotonic interactions between ventricular myocytes and fibroblasts. Biophys. J 2007;92:4121–4132. [PubMed: 17307821]

Maleckar MM, Greenstein JL, Giles WR, Trayanova NA. Mechanisms of rate dependence in an updated model of the human atrial myocyte. Am. J. Physiol. submitted for publication-a.

Maleckar MM, Greenstein JL, Giles WR, Trayanova NA. Electrotonic coupling between human atrial myocytes and fibroblasts alters myocyte excitability and repolarization. Biophys. J. submitted for publication-b.

Miragoli M, Gaudesius G, Rohr S. Electrotonic modulation of cardiac impulse conduction by myofibroblasts. Circ. Res 2006;98:801–810. [PubMed: 16484613]

Nattel S, Opie LH. Controversies in atrial fibrillation. Lancet 2006;367:262–272. [PubMed: 16427496]

Ninomiya I. Direct evidence of nonuniform distribution of vagal effects on dog atria. Circ. Res 1966;19:576–583. [PubMed: 5925156]

Nygren A, Fiset C, Firek L, Clark JW, Lindblad DS, Clark RB, Giles WR. Mathematical model of an adult human atrial cell: the role of K^+ currents in repolarization. Circ. Res 1998;82:63–81. [PubMed: 9440706]

Nygren A, Leon LJ, Giles WR. Simulations of the human atrial action potential. Phil. Trans. R. Soc. Lond. A 2001;359:1111–1125.

Oliver PM, Fox JE, Kim R, Rockman HA, Kim HS, Reddick RL, Pandey KN, Milgram SL, Smithies O, Maeda N. Hypertension, cardiac hypertrophy, and sudden death in mice lacking natriuretic peptide receptor A. Proc. Natl. Acad. Sci. U.S.A 1997;94:14730–14735. [PubMed: 9405681]

Pappano AJ, Mubagwa K. Muscarinic agonist-induced actions on potassium and calcium channels in atrial myocytes: differential desensitization. Eur. Heart J 1991;12:70–75. [PubMed: 1666556]

Pijnappels DA, van Tuyn J, Devries AAF, Grauss RW, van der Laarse A, Ypey DL, Atsma DE, Chalij MJ. Resynchronization of separated rat cardiomyocyte fields with genetically modified human ventricular scar fibroblasts. Circulation 2007;116:2018–2028. [PubMed: 17938287]

Ramirez RJ, Nattel S, Courtemanche M. Mathematical analysis of canine atrial action potentials: rate, regional factors, and electrical remodeling. Am. J. Physiol. Heart Circ. Physiol 2000;279:H1767–H1785. [PubMed: 11009464]

Rampe D, Wible B, Fedida D, Dage RC, Brown AM. Verapamil blocks a rapidly activating delayed rectifier K+ channel cloned from human heart. Mol. Pharmacol 1993;44:642–648. [PubMed: 8371716]

Rook MB, van Ginnekin AC, de Jonge B, el Aoumari A, Gros D, Jongsma HJ. Differences in gap junction channels between cardiac myocytes, fibroblasts, and heterologous pairs. Am. J. Physiol 1992;263:C959–C977. [PubMed: 1279981]

Rose RA, Hatano N, Ohya S, Imaizumi Y, Giles WR. C-type natriuretic peptide activates a non-selective cation current in acutely isolated rat cardiac fibroblasts via natriuretic peptide C receptor-mediated signalling. J. Physiol 2007;580:255–274. [PubMed: 17204501]

Rose RA, Giles WR. Natriuretic peptide C receptor signaling in the heart and vasculature. J. Physiol 2008;586:353–366. [PubMed: 18006579]

Sachse FB, Moreno AP, Abildskov JA. Electrophysiological modeling of fibroblasts and their interaction with myocytes. Ann. Biomed. Eng 2008;36:41–56. [PubMed: 17999190]

Schuessler RB, Grayson TM, Bromberg BI, Cox JL, Boineau JP. Cholinergically mediated tachyarrhythmias induced by a single extrastimulus in the isolated canine right atrium. Circ. Res 1992;71:1254–1267. [PubMed: 1394883]

Shibata EF, Brown TLY, Washburn ZW, Bai J, Revak TJ, Butters CA. Autonomic regulation of voltage-gated cardiac ion channels. J. Cardiovasc. Electrophysiol 2006;17:S34–S42. [PubMed: 16686680]

Shibata EF, Drury T, Refsum H, Aldrete V, Giles W. Contributions of a transient outward current to repolarization in human atrium. Am. J. Physiol 1989;257:H1773–H1781. [PubMed: 2557769]

Shibukawa Y, Chilton EL, MacCannell KA, Clark RB, Giles WR. K+ currents activated by depolarization in cardiac fibroblasts. Biophys. J 2005;88:3924–3935. [PubMed: 15764658]

Shiroshita-Takeshita A, Bianca JJ, Brundel M, Nattel S. Atrial fibrillation: basic mechanisms, remodeling and triggers. J. Card. Electrophysiol 2005;13:181–193.

Spach MS, Boineau JP. Microfibrosis produces electrical load variations due to loss of side-to-side cell connections: a major mechanism of structural heart disease arrhythmias. Pacing Clin. Electrophysiol 1997;20:397–413. [PubMed: 9058844]

Spach MS, Miller WT 3rd, Geselowitz DB, Barr RC, Kootsey JM, Johnson EA. The discontinuous nature of propagation in normal canine cardiac muscle. Evidence for recurrent discontinuities of intracellular resistance that affect the membrane currents. Circ. Res 1981;48:39–54. [PubMed: 7438345]

VanWagoner DR, Nerbonne JM. Molecular basis of electrical remodeling in atrial fibrillation. J. Mol. Cell Cardiol 2000;32:1101–1117. [PubMed: 10888261]

Wang S, Bondarenko VE, Qu YJ, Bett GC, Morales MJ, Rasmusson RL, Strauss HC. Time- and voltage-dependent components of Kv4.3 inactivation. Biophys. J 2005;89:3026–3041. [PubMed: 16100281]

Wang Y, Xu H, Kumar R, Tipparaju SM, Wagner MB, Joyner RW. Differences in transient outward current properties between neonatal and adult human atrial myocytes. J. Mol. Cell Cardiol 2003;35:1083–1092. [PubMed: 12967631]

Zlochiver S, Muñoz V, Vikstrom KL, Taffet SM, Berenfeld O, Jalife J. Electrotonic myofibroblast-to-myocyte coupling increases propensity to reentrant arrhythmias in two-dimensional cardiac monolayers. Biophys. J 2008;95:446–4480.

List of symbols

APA	action potential amplitude
APD_{90}	action potential duration at 90% repolarization
B	background
Ca,P	sarcolemmal Ca^{2+} pump
CBC	carbamylcholine
dV/dt_{max}	maximum rate of change of voltage during action potential
E	reversal potential
Fb	fibroblast
G	conductance
gap	gap junctional
I	current
K(ACh)	acetylcholine-activated K^+ channel
kur, K1, Kr, Ks	K^+ current species
NaCa	Na^+–Ca^{2+} exchanger
NaK	Na^+–K^+ pump
NP	natriuretic peptides
Φ_{en}	electroneutral Na^+ influx
RMP	resting membrane potential
t	transient outward
V	membrane potential

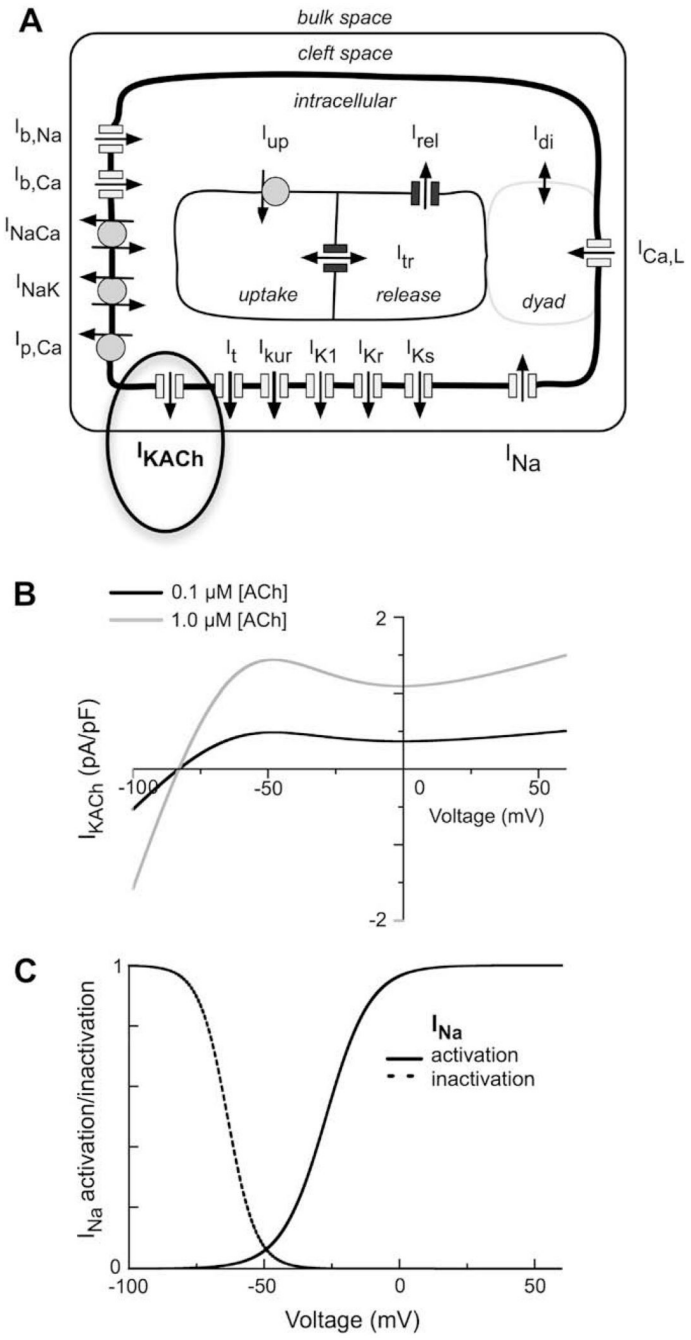

Fig. 1.

Diagram of the equivalent circuit components of our mathematical model of the human atrial myocyte action potential. (A) A schematic of the time- and voltage-gated membrane currents, ion pumps and exchangers, as well as the ligand-gated K^+ current, $I_{K(ACh)}$, activated by muscarinic agonists. (B) *I–V* relationships of $I_{K(ACh)}$ corresponding to two different concentrations of either acetylcholine (ACh). (C) Steady-state activation (solid line) and inactivation (dashed line) relationships for I_{Na} in this model of the human atrial myocyte.

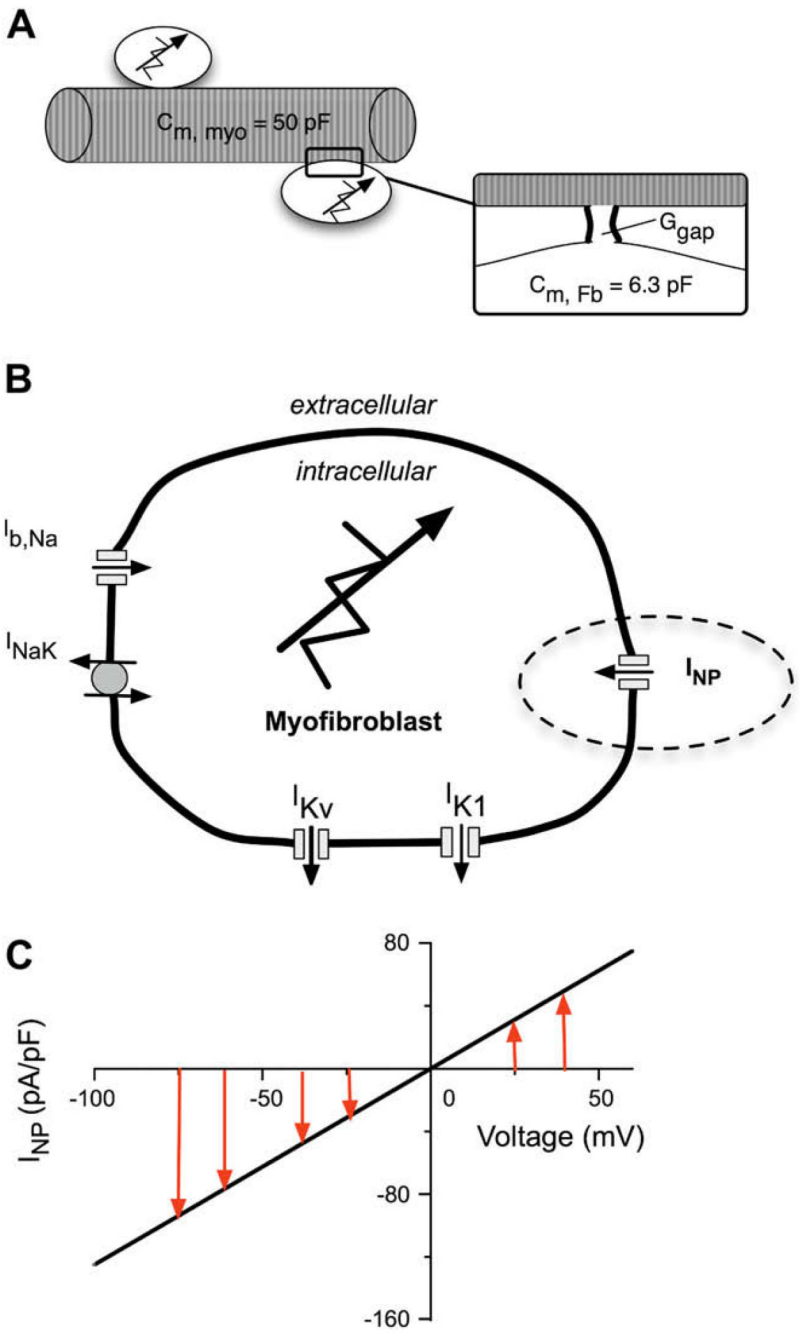

Fig. 2.

Schematic diagram of the coupled human atrial myocyte/fibroblast paradigm which forms the basis of this study. (A) One human atrial myocyte was coupled to one fibroblast modeled according to (MacCannell et al., 2007), and assuming a gap junctional conductance, G_{gap} of 0.5 nS. The total capacitance of the human atrial myocyte is 50 pF and the capacitance of the fibroblast is 6.3 pF. (B) A schematic of the fibroblast which incorporates five active membrane conductances. The voltage-gated currents are a background Na^+ current, $I_{b,Na}$; two K^+ currents, I_{K1}, and I_{Kv}; the Na^+–K^+ pump current I_{NaK}. I_{NP} represents the novel ligand-gated transient receptor protein (TRP) channel current which is activated by natriuretic peptide. (C) The *I–V*

curve for the natriuretic peptide-induced conductance in the fibroblast. Note, the linear relationship having a reversal potential near 0 mV.

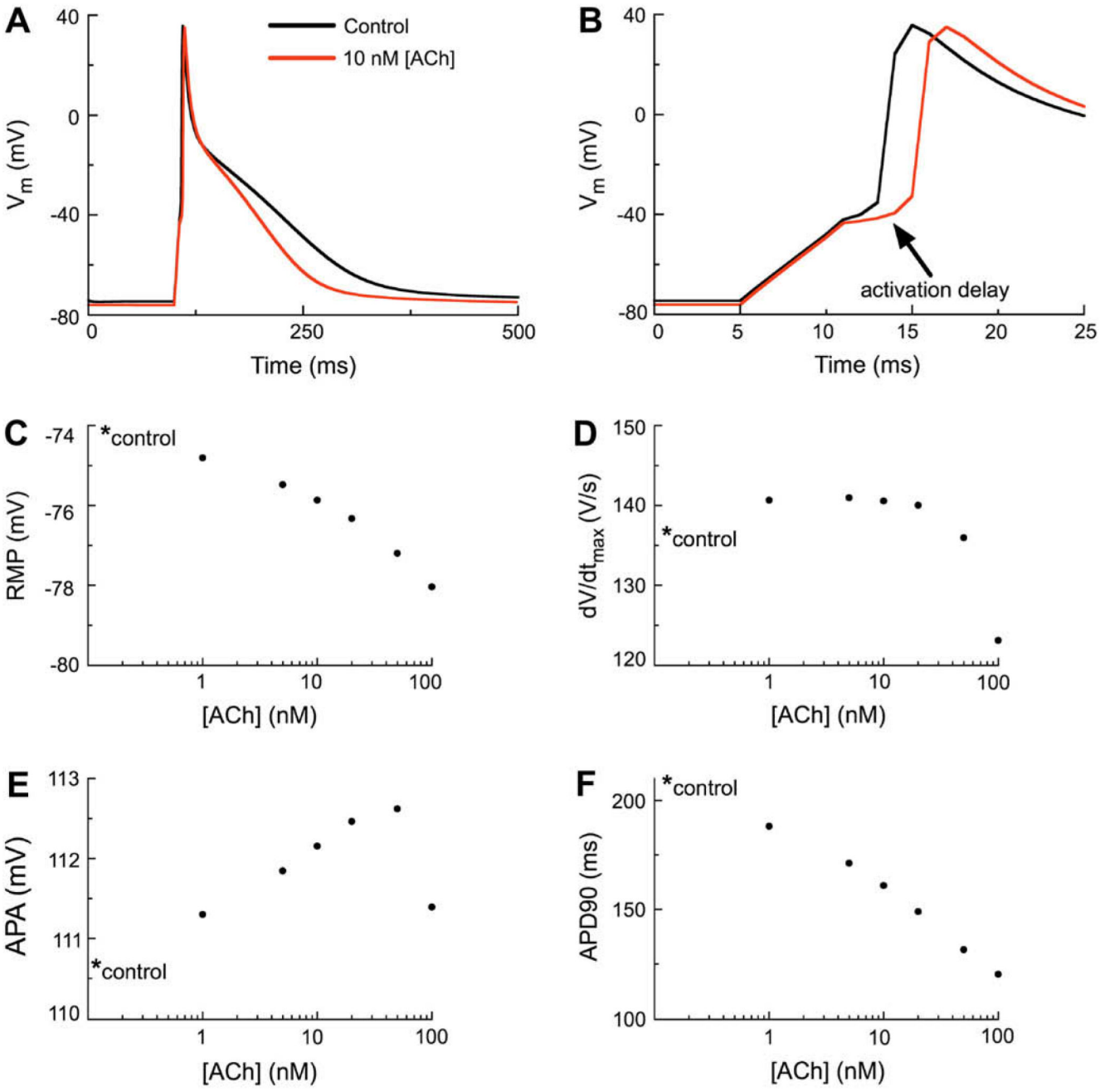

Fig. 3.

The effects of $I_{K(ACh)}$ on the human atrial action potential waveform. (A) Simulated action potentials (APs) corresponding to the control (no $I_{K(ACh)}$) and to superfusion with 10 nM ACh (data shown in red). The stimulation protocol employed a 310 pA stimulus current lasting 6 ms at a basic cycle length of 1 s (1 Hz). As shown by the red trace, activation of $I_{K(ACh)}$ hyperpolarizes the resting membrane potential (RMP) and abbreviates the action potential duration (APD). (B) Note that 10 nM ACh results in delayed activation of the human atrial myocyte AP (indicated by arrow). However, there is no decrease in the amplitude of the delayed AP. (C) Concentration–response relationship for [ACh] vs. RMP in the human atrial myocyte. In this and all subsequent panels the control value is marked with an asterisk. (D)

Concentration–response relationship of [ACh] vs. dV/dt_{max} of the human atrial myocyte. (E) Concentration–response relationship of [ACh] vs. action potential amplitude (APA) of the human atrial myocyte. (F) Concentration–response relationship of [ACh] vs. action potential duration at 90% repolarization (APD90) of the human atrial myocyte.

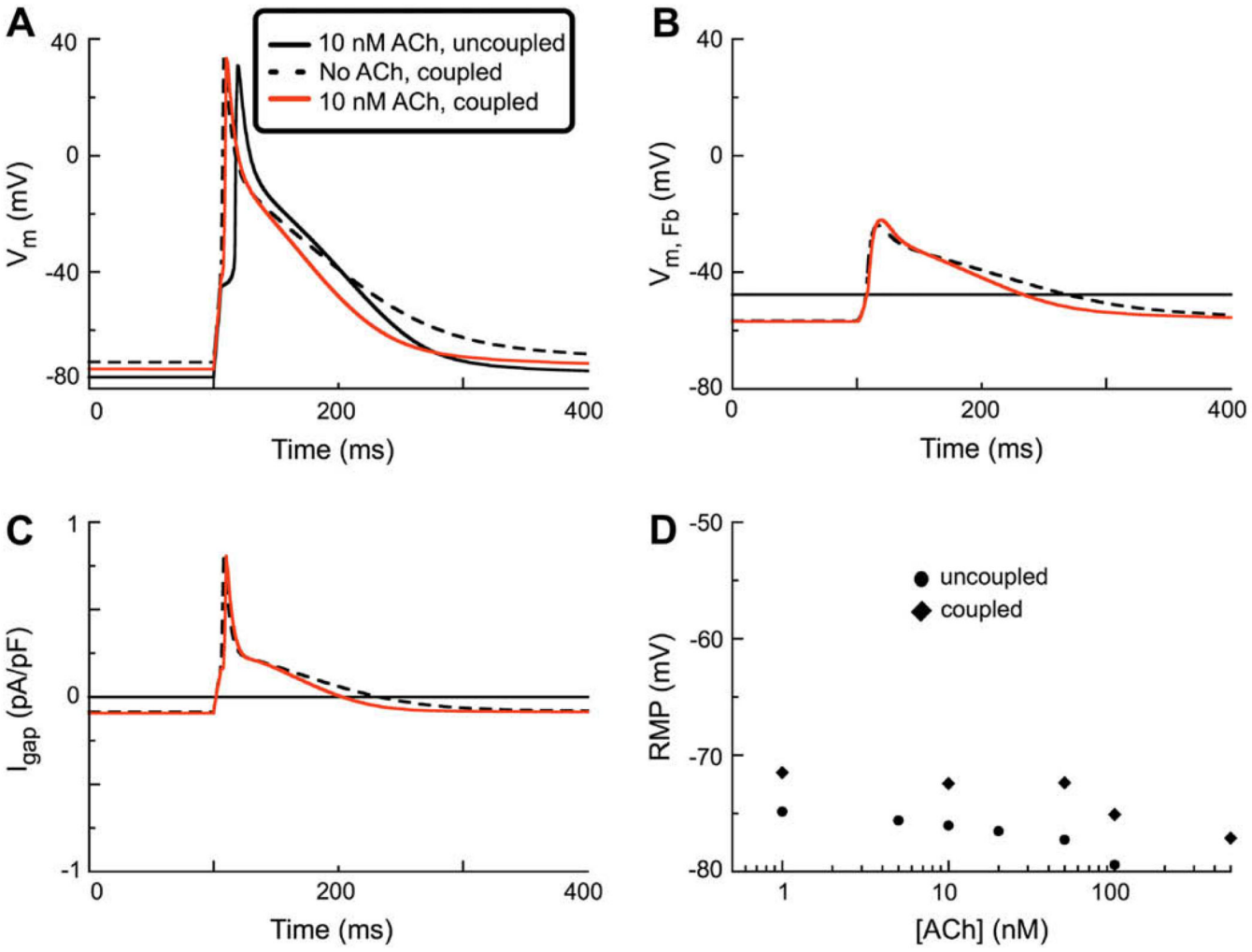

Fig. 4.

Action potential simulations made on the basis of a model system consisting of one human atrial myocyte (incorporating $I_{K(ACh)}$ at 10 nM) coupled to a one fibroblast through a G_{gap} of 0.5 nS. (A) Comparison of AP waveforms during a stimulation protocol employing a 6 ms 280 pA stimulus current applied a basic cycle length of 1 s (1 Hz). Note that in the uncoupled myocyte when $I_{K(ACh)}$ (black solid trace) is activated there is an activation delay. In contrast, since coupling the ACh-treated myocyte to a fibroblast depolarizes the RMP, application of ACh does not result in any activation delay in this situation (red line). Note that the coupled myocyte which is not treated with ACh has the most depolarized RMP, and a relative prolongation of APD (black dashed line). (B) Comparison of the electrotonic changes in the membrane potential of the fibroblast (V_{Fb}) as a result of coupling to one atrial myocyte. Solid black line represents the intrinsic or control RMP of the uncoupled fibroblast. Coupling to a myocyte (either with or without $I_{K(ACh)}$) results in a similar hyper-polarization of the fibroblast RMP. (C) Gap junctional current, *I*gap. Note that coupling one fibroblast to one myocyte either with or without $I_{K(ACh)}$, results in a similar I_{gap}. (D) Concentration–response relationship for [ACh] vs. RMP in both the uncoupled (●) and coupled (◊) human atrial myocyte. The ligand-gated current, $I_{K(ACh)}$, was active during each of these simulations in the myocyte model (black circles and diamonds, respectively).

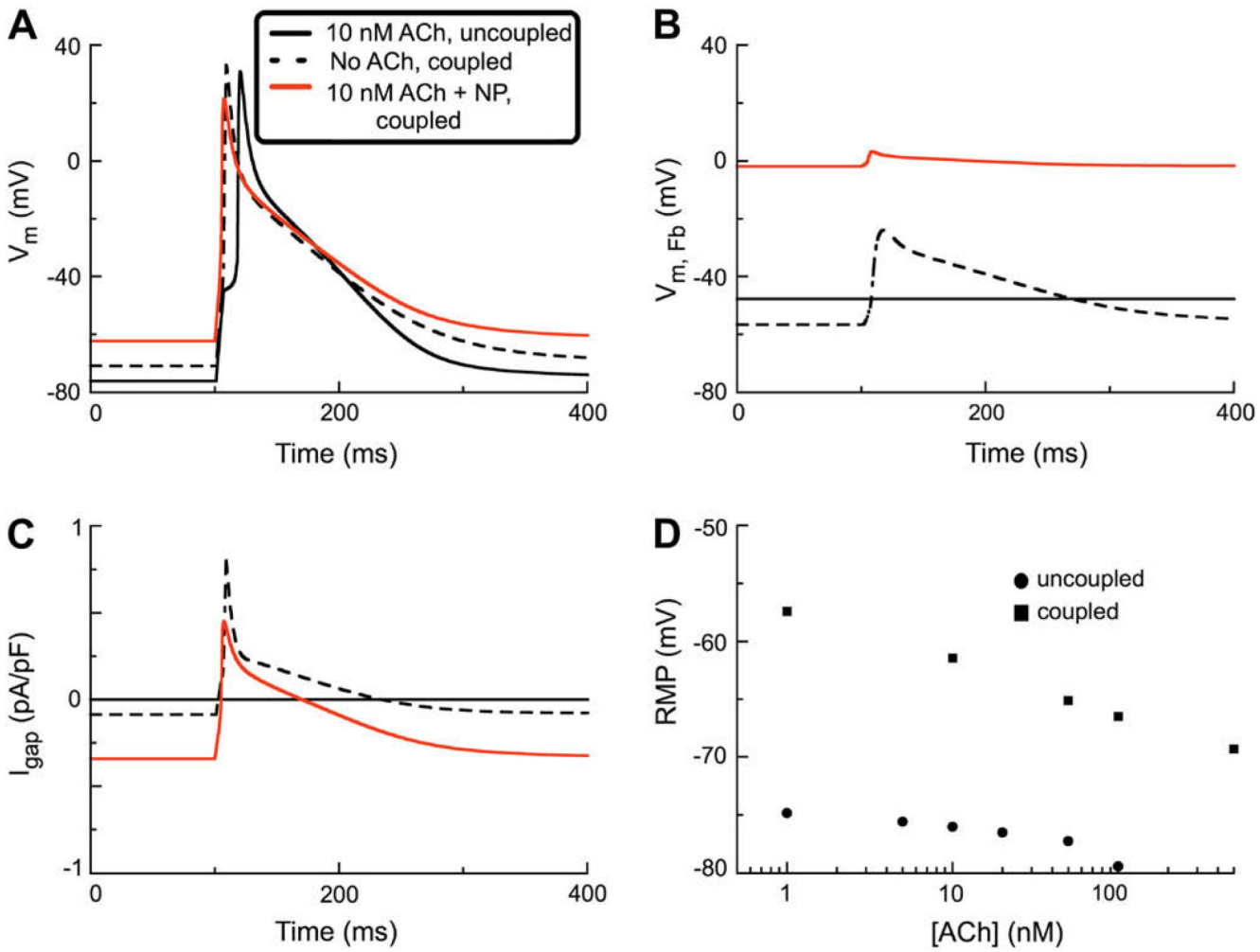

Fig. 5.

Simulations of the human atrial action potential in a coupled myocyte/fibroblast system with both $I_{K(ACh)}$ and I_{NP} activated. The stimulus current (280 pA, 6 ms) was applied at 1 Hz and a fixed coupling resistance (0.5 nS) was assumed. A The action potential waveform denoted by the solid black trace illustrates the effect of activation of the $I_{K\text{-}ACh}$ in this situation which assumed no intercellular coupling. Note the increased latency, or delay, in the firing of the AP. In this panel the superimposed red trace shows the changes produced by electrotonic coupling to one fibroblast in which I_{NP} is activated. Note: (i) depolarization of the RMP, and (ii) prolongation of the APD. The dashed line shows the AP waveform assuming no activation of $I_{K\text{-}ACh}$, in the presence of I_{NP} in one coupled fibroblast. B shows the corresponding changes in the fibroblast membrane potential V_{Fb}. Solid black line: control RMP in fibroblast (no coupling). Note that activation of I_{NP} causes a large depolarization (red trace). The dashed line is the V_{FB} with $I_{K(ACh)}$ and I_{NP} activated. C shows the gap junction current under the three conditions chosen: black trace – resting, control fibroblast; red trace – I_{NP} activated; dashed trace – both $I_{K(ACh)}$ and I_{NP} activated. D Two concentration–response relationships for RMP vs. [ACh]. The black circles (●) show the effect of activation of $I_{K\text{-}ACh}$ on RMP in an uncoupled atrial myocyte (see also Fig. 3). The black squares (■) are analogous data from simulations assuming (i) myocyte–fibroblast coupling (0.5 nS); and (ii) activation of I_{NP} in the fibroblast.